Published by Elsevier Science Inc.

ISSN 0735-1097/03/$30.00
PII S0735-1097(02)02623-2

Ablation of Electrograms With an Isolated, Delayed Component as Treatment of Unmappable Monomorphic Ventricular Tachycardias in Patients With Structural Heart Disease

Angel Arenal, MD, Esteban Glez-Torrecilla, MD, Mercedes Ortiz, PHD, Julian Villacastín, MD, Javier Fdez-Portales, MD, Elena Sousa, MD, Silvia del Castillo, MD, Leopoldo Perez de Isla, MD, Javier Jimenez, MD, Jesus Almendral, MD

Madrid, Spain

OBJECTIVES We sought to evaluate the feasibility of identifying and ablating the substrate of unmappable ventricular tachycardia (VT).

BACKGROUND Noninducible and nonstable VT cannot be ablated by the conventional approach.

METHODS We studied 24 patients with documented monomorphic VT. Twenty-one patients had ischemic cardiomyopathy, two had nonischemic cardiomyopathy, and one had tetralogy of Fallot. Twelve patients had an implantable cardioverter-defibrillator. Conventional activation mapping was not possible in 18 patients: at least 1 of the clinical VTs or the clinical VT was not inducible in 12 patients, and VT was not tolerated in 6 patients. This group had experienced between 1 and 106 VT episodes in the month before the ablation procedure. Endocardial electroanatomic activation maps (Carto System) during sinus rhythm (SR) and right ventricular apex (RVA) pacing were obtained to define areas for which an electrogram displayed isolated, delayed components (E-IDC). These electrograms were characterized by double or multiple components separated by ≥50 ms.

RESULTS One area of E-IDC was recorded in 20 patients, and 2 or more were recorded in 4 patients. In 23 patients, these areas were detected during RVA pacing; in only 14 during SR. An E-IDC area related to the clinical VT was identified in each patient. Ablation guided by E-IDC suppressed all but one clinical VT whose inducibility suppression was tested. During a follow-up period of 9 ± 4 months, three patients had recurrences of the ablated VT and two of a different VT.

CONCLUSIONS Electrograms with IDCs related to clinical VT can be identified in the majority of patients during RVA pacing. Radiofrequency ablation of E-IDC seems effective in controlling unmappable VT. (J Am Coll Cardiol 2003;41:81–92) © 2003 by the American College of Cardiology Foundation

Slow conduction areas are part of the substrate of the reentrant circuits in most sustained monomorphic ventricular tachycardias (SMVTs) occurring in patients with structural heart disease (1). This part of the reentrant circuit has been classically characterized by the recording of presystolic isolated electrograms during tachycardia (2–8). The identification of this component of the circuit requires careful and time-consuming endocardial mapping, a procedure that is not feasible in noninducible or nontolerated ventricular tachycardia (VT). Slow conduction takes place on the border of the scar tissue; therefore, abnormal and low amplitude electrograms have been recorded during sinus rhythm (SR) at these sites. As low-amplitude electrograms are recorded all along the scarred endocardial surface, they have low specificity for VT substrate identification (9). We hypothesized that the recording of electrograms displaying an isolated, delayed component (E-IDC), characterized by double or multiple components separated by very-low-amplitude signals or isoelectric intervals, could better identify SMVT related slow conduction areas than low-amplitude electrograms. Nevertheless, fractionated and late electrograms are rarely recorded during SR (10). Overlapping of electrograms or a particular orientation of a line of block with respect to the activation front may preclude the identification of multiple components during SR; this limitation can be overcome by changing the activation front (11–13). We presumed that a different propagation front, such as during right ventricular apex (RVA) pacing, could identify E-IDCs otherwise not detected.

The purpose of this study was to assess: 1) the incidence, location, and extension of E-IDC in patients with clinical SMVT and structural heart disease; 2) the feasibility of relating E-IDC to documented clinical SMVT; and 3) the efficacy of E-IDC ablation as treatment of noninducible and/or nontolerated VT.

METHODS

Population. In this protocol, approved by the Research and Ethical Committee of our institution, we included 24 of 38 consecutive patients with structural heart disease and SMVT documented by the 12-lead electrocardiogram

From the Department of Cardiology, Hospital General Universitario Gregorio Marañón, Madrid, Spain.

Manuscript received February 7, 2002; revised manuscript received September 10, 2002, accepted September 20, 2002.

Abbreviations and Acronyms

E-IDC = electrogram displaying isolated, delayed component
E-LIDC = electrogram displaying latest isolated, delayed component
E-QRS = electrogram's QRS interval
ICD = implantable cardioverter-defibrillator
RFA = radiofrequency ablation
RVA = right ventricular apex
SMVT = sustained monomorphic ventricular tachycardia
S-QRS = stimulus to QRS interval
SR = sinus rhythm
VT = ventricular tachycardia

(ECG) who were referred for radiofrequency ablation (RFA).

Conventional treatment was considered not suitable in 18 patients (Patient nos. 1 to 18) (Table 1). Twelve patients were considered as noninducible because no clinical VT (n = 9) or the most recently recorded VT and that responsible for the multiple episodes was not induced (n = 3: patient nos. 4, 9, and 17). In six additional patients, the induced clinical VT was not tolerated.

The remaining six patients (Patient nos. 19 to 24) (Table 1) with a clinically inducible and well-tolerated VT were included to: 1) obtain activation maps during SR/RVA pacing and during VT; and 2) compare the successful ablation site, guided by activation and entrainment mapping criteria, with the limits of the E-IDC area.

Seventeen patients had multiple VT episodes despite the use of amiodarone or sotalol. In seven patients, despite few VT episodes, RFA was the first option of treatment, according to our policy of offering RFA when: 1) the VT remained unnoticed due to the slow rate until heart failure appeared; 2) patients refused to follow long-term antiarrhythmic treatment; and 3) it was adjuvant therapy to implantable cardioverter-defibrillator (ICD) placement when the VT was rapidly syncopal and we presumed the ICD could not terminate the VT before the appearance of syncope.

Study protocol (Fig. 1). ELECTROPHYSIOLOGIC STUDY. After written, informed consent was obtained, an electrophysiologic study was performed in the post-absorptive state. At least two or three quadripolar catheters were placed at the right atrium, His bundle area, RVA, or right ventricular outflow tract. The distal pair of electrodes was used for pacing, and the proximal pair for local electrogram recording. Intracardiac recordings were filtered at 30 to 500 Hz and displayed simultaneously with four to six ECG leads at a paper speed of 100 to 200 mm/s on a 12-channel recorder (Midas, Hellige Biomedical, Freiburg, Germany). Stimulation was performed with a programmable stimulator (UHS-20 Biotronik, Berlin, Germany) set to deliver rectangular pulses of 2-ms duration at twice the diastolic threshold. Programmed stimulation was performed to induce VT through triple extrastimuli at two right ventricular sites.

Mapping of the left and right ventricles: location of E-IDC. Detailed endocardial mapping was performed during SR and during pacing at RVA at 600 ms. In 22 patients, mapping and ablation were performed using the Carto (Biosense-Webster, Waterloo, Belgium) magnetic mapping system with the Navistar catheter. The Navistar bipole consists of a 4-mm-tip electrode and 2-mm-ring electrode separated by 1 mm of spacing. Bipolar electrograms were filtered at 30 to 400 Hz and displayed at 100 mm/s; peak-to-peak amplitude was measured automatically. The magnetic mapping system includes a magnetic sensor in the catheter tip that can be localized in a three-dimensional space using the ultra-low-frequency magnetic field generators placed under the fluoroscopic table. This system permits three-dimensional reconstruction of the endocardium, which can be shown on a computer display (14,15).

To define the limits of the area demonstrating E-IDC, once an E-IDC was identified, multiple sites were explored around it to obtain a distance of ≤1 cm between the mapped sites. The E-IDCs were labeled for rapid location on the maps. Activation maps were reconstructed taking the peak of the largest deflection of every single electrogram as the local activation time.

The Carto system can display the amplitude of bipolar electrograms as voltage maps. When multiple-component electrograms were recorded, the voltage of the largest component was automatically selected. The color display on the voltage map was set to a color range of 0.5 to 1.5 mV to distinguish the limits of the scar. We differentiated between: 1) complete scar, displayed in gray, characterized by electrograms with a voltage amplitude ≤0.1 mV; and 2) dense scar, displayed in red, with an electrographic amplitude ≥0.1 and ≤0.5 mV. We measured the distance between the E-IDC area limit and the closest border of the dense scar to determine whether RFA lesions could affect normal myocardium or whether a hypothetical ablation line along the border of the scar could have eliminated the E-IDC.

Clinical VT and E-IDC. After the maps were completely depicted, in order to relate a particular E-IDC area to clinical VT, pace mapping was performed starting at the electrogram showing the latest isolated, delayed component (E-LIDC). When the QRS morphology in clinical VT was not reproduced from the E-LIDC, VT morphology was analyzed and a site from the limits of the E-IDC area was selected for pacing. After an identical or similarly paced QRS interval, defined by the same R/S ratio in all leads, was obtained, we proceeded to induce VT.

We assumed a relationship between E-IDC and clinical VT when the following criteria were met: 1) noninducible VT: pace mapping reproducing the QRS morphology in clinical VT and the stimulus to QRS interval (S-QRS) >50 ms; 2) inducible but poorly tolerated VT: presence of a pre-systolic or mid-diastolic electrogram and a difference

Table 1. Patient Characteristics

Patient No.	Age (yrs)/ Gender	Heart Disease	LVEF (%)	ICD	CVT (ms)	Episodes	IVT (ms)	LCT
1	67/M	IC	25	+	RRS (370)	36/month	—	NI
2	69/F	DCM	20	−	RRS (400)	10/week	—	NI
					RLS (450)		—	
3	74/M	IC	40	−	RLS (320)	1	RLS (310)	NT
4	65/M	IC	30	−	RRI (340)	Multiple/week	—	NI
					RRS (350)		RRS (370)	
5	67/M	IC	25	−	RRS (300)	1	RRS (300)	NT
6	56/M	IC	30	+	RLS (400)	94/month	—	NI
7	58/M	IC	34	−	LRI (300)	1	LRI (300)	NT
8	68/M	IC	55	−	RLS (280)	1	RLS (280)	NT
9	72/M	IC	35	−	RRS (400)	Multiple/week	—	NI
					RLS (380)		—	
					RLI (400)		RLI (480)	
10	72/M	IC	25	+	RRS (380)	11/month	—	NI
11	74/M	IC	25	−	RLS (320)	1	RLS (310)	NT
							LLS (300)	
12	59/M	DCM	25	+	RRS (360)	16/month	RRS (380)	NS
							RLS (280)	
13	28/M	TF	55	−	RRI (440)	3/month	LLS (430)	NI
14	71/M	IC	20	+	LRI (420)	25/month	—	NI
15	73/M	IC	40	+	RRS (380)	3/month	—	NI
16	73/M	IC	20	−	LRI (360)	1/month	LLS (270)	NI
17	67M	IC	20	−	RRS (420)	55/month		NI
					RLS (380)		RRS (400)	
					RRS (400)		RRI (400)	
18	64/M	IC	30	+	RRS (400)	1/month	—	NI
19	72/F	IC	27	−	RRS (360)	10/week	RRS (380)	
							LLS (400)	
20	51/M	IC	35	+	RRI (350)	6/week	RRI (350)	
21	70/M	IC	25	+	LLI (500)	5/week	LLI (540)	
22	71/M	IC	45	+	RLS (480)	106/month	RLS (480)	
							RLI (400)	
23	72/M	IC	35	+	LLS (400)	4/week	LLS (380)	
24	74/M	IC	30	+	RRS (420)	29/month	RRS (440)	
Mean ± SD	66 ± 9		30 ± 9					

CVT = clinical ventricular tachycardia; DCM = dilated cardiomyopathy; F = female; IC = ischemic cardiomyopathy; ICD = implantable cardioverter-defibrillator; IVT = induced ventricular tachycardia; LCT = limitation of conventional treatment; LVEF = left ventricular ejection fraction; LLI = left bundle branch block left inferior axis; LLS = left bundle branch block left superior axis; LRI = left bundle branch block right inferior axis; M = male; NI = noninducible; NS = nonstable; NT = nontolerated; RLI = right bundle branch block left inferior axis; RLS = right bundle branch block left superior axis; RRI = right bundle branch block right inferior axis; RRS = right bundle branch block right superior axis; TF = tetralogy of Fallot.

≤30 ms between the electrogram's QRS interval (E-QRS) in VT and S-QRS when the preceding pace map was similar; and 3) well-tolerated VT: presence of a pre-systolic or mid-diastolic electrogram, concealed entrainment, and a first post-pacing interval–VT cycle length difference ≤30 ms.

Radiofrequency ablation. Radiofrequency energy was delivered as a continuous, unmodulated sine wave of 500 kHz between the distal electrode of the ablation catheter and a large skin electrode on the posterior chest.

The conventional RFA approach was followed in the six patients (Patient nos. 19 to 24) (Table 1) in whom clinical VT was induced and tolerated; radiofrequency energy was only delivered at sites identified by conventional entrainment mapping criteria.

In Patients 1 to 18, in whom clinical VT was unmappable, an E-IDC area was considered as a RFA target, and all E-IDC sites were ablated provided that: 1) pace mapping from any E-IDC site, usually the E-LIDC, in the area reproduced the target clinical VT with S-QRS >50 ms; or 2) any E-IDC became mid-diastolic during VT induction. The induction of a different VT, even if it was tolerated, did not modify the RFA approach, provided that no mid-diastolic electrogram during VT was recorded outside the E-IDC area. The target temperature was 60°C. All lesions were delivered for at least 1 min, unless a rise in impedance was noted.

The end points of the procedure were: 1) disappearance of all IDCs of a clinical VT-related area in those patients with unmappable VT; and 2) inducibility suppression of clinical VT. Heparin was infused throughout the procedure. To those patients in whom VT was not inducible or inducibility suppression was not tested, ICD implantation was advocated.

Definitions. E-IDC. Electrograms recorded in the scar tissue showing double or multiple components separated >50 ms

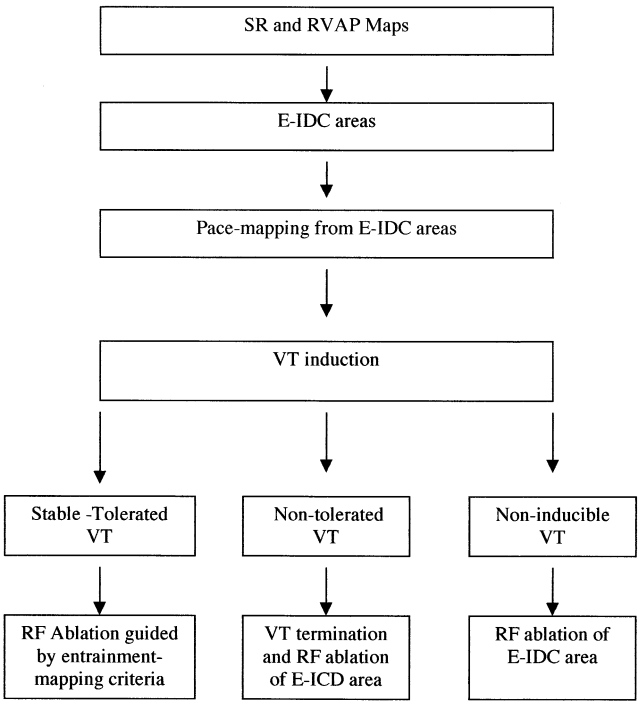

Figure 1. Diagram showing the approach to mapping and radiofrequency (RF) ablation of ventricular tachycardia (VT). E-IDC = electrogram displaying isolated, delayed component; RVAP = right ventricular apex pacing; SR = sinus rhythm.

by very low amplitude signals or an isoelectric interval. During RVA pacing, the activation time of the latest component from the stimulus artifact had to be >150 ms.

E-QRS. During VT, this was the interval from the mid-diastolic electrogram to the following QRS onset.

E-LIDC. This was considered as the E-IDC showing the longest activation time to the last component either from the QRS onset during SR or the stimulus artifact during RV pacing.

POST-PACING INTERVAL–VT CYCLE LENGTH DIFFERENCE. This was the difference between the post-pacing interval and the tachycardia cycle length.

S-QRS. This was the interval from the stimulus to the onset of the following QRS complex during pacing from the E-LIDC.

S-QRS–E-QRS DIFFERENCE. This was the difference between the S-QRS interval during pacing from the E-LIDC on SR and the E-QRS interval during VT.

E-IDC AREA. This was the area circumscribing the sites where E-IDC were recorded; we considered the presence of a distinct area when the distance between the closest E-IDCs was >20 mm due to the presence of normal or scar tissue.

Statistical analysis. Data are expressed as the mean value ± SD. Comparisons were performed using the Student *t* test and Fisher exact test. A probability value of 0.05 was considered significant.

Table 2. Mapping Characteristics

	E-IDC Areas			
Patient No.	E-IDC Loc.	E-IDC Recording	I-LIDC (RVAP/SR) (ms)	E-IDC With >2 Components (RVAP/SR)
1	1	RVAP/SR	270/250	+/+
2	7-1	RVAP	260/—	+
3	6-8	SR	—/130	+
4	5-7	RVAP/SR	240/300	+/+
5	8	RVAP	200/—	+
6	5-6	RVAP/SR	280/200	+/+
7	2-3	RVAP/SR	250/140	+/+
8	5-6	RVAP/SR	190/130	+/+
9	6-8	RVAP	250/—	+
10	1-2-11	RVAP	230/—	+
11	6	RVAP	210/—	+
12	7-8	RVAP	220/—	−
13	1	RVAP/SR	180/80	+/+
14	1-2	RVAP	150/—	+
15	6-8	RVAP	180/—	+
16	1-11	RVAP	200/—	+
17	1-9-11	RVAP/SR	230/140	+/+
18	1-2	RVAP/SR	245/110	+/+
	11-3*	RVAP/SR	260/110	+/+
19	1-2	RVAP/SR	160/180	−/−
	11-9*	RVAP/SR	150/140	−/−
20	8-10	RVAP	230/—	+
21	3	RVAP	240/—	+
	1*	RVAP	220/—	+
22	8-10	RVAP/SR	280/190	+/+
23	6	RVAP	220	+
24	7	RVAP/SR	220/140	+/+
	5*	RVAP	190/—	+
	10*	RVAP	200/—	+
Mean ± SD			220 ± 34/143 ± 54	

*E-IDC areas that were not related to any clinical ventricular tachycardia.

E-IDC = electrogram with isolated, delayed component; I-LIDC = interval between the stimulus artifact or QRS onset and the latest isolated delayed component; Loc. = ventricular segment location of E-IDC (mapping schema in ref. 10); RVAP = right ventricular apex pacing; SR = sinus rhythm.

RESULTS

Table 1 shows the characteristics of clinical and induced VT.

Endocardial maps: E-IDC location (Table 2). Ventricular maps were constructed using 111 ± 27 points (range 70 to 146). Twenty-nine E-IDC areas were detected: 12 were defined in 12 of 22 patients during SR (2 patients underwent permanent pacing); 11 of these areas were also detected during RVA pacing. The remaining 17 E-IDC areas were only detected during RVA pacing. Therefore, the E-IDC was detected in 12 of 22 patients during SR and in 23 of 24 patients during RVA pacing ($p < 0.01$) (Fig. 2). Four patients (nos. 18, 19, 21, and 24) had two or three different areas; the remaining patients had only one. An E-IDC with more than two components was recorded in 26 of 29 E-IDC areas and in 24 of 26 areas in 21 patients with ischemic heart disease. The following data were obtained during RVA pacing. Extension of the E-IDC area (3.5 ± 2.6 cm^2 [range 1 to 12]) was smaller than the area with a

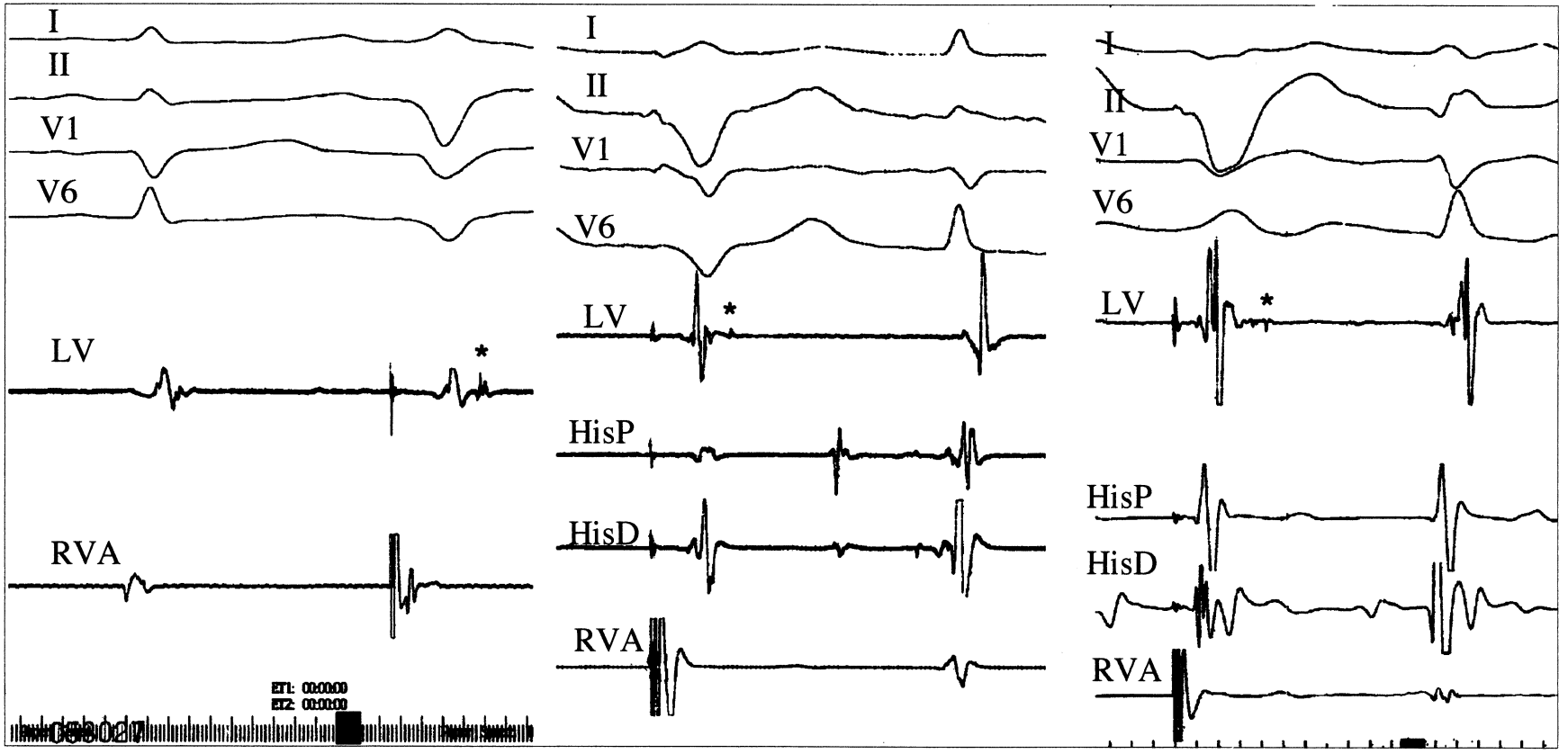

Figure 2. Three examples in which the E-IDCs were recorded only during RVA pacing. Four ECG surface leads are recorded, along with intracardiac electrograms from the His area, RVA, and left ventricle (LV) during RVA pacing and SR. Notice that in the three examples, during RVA pacing, a small and late component separated by an isoelectric line appears. This component is not evident during SR.

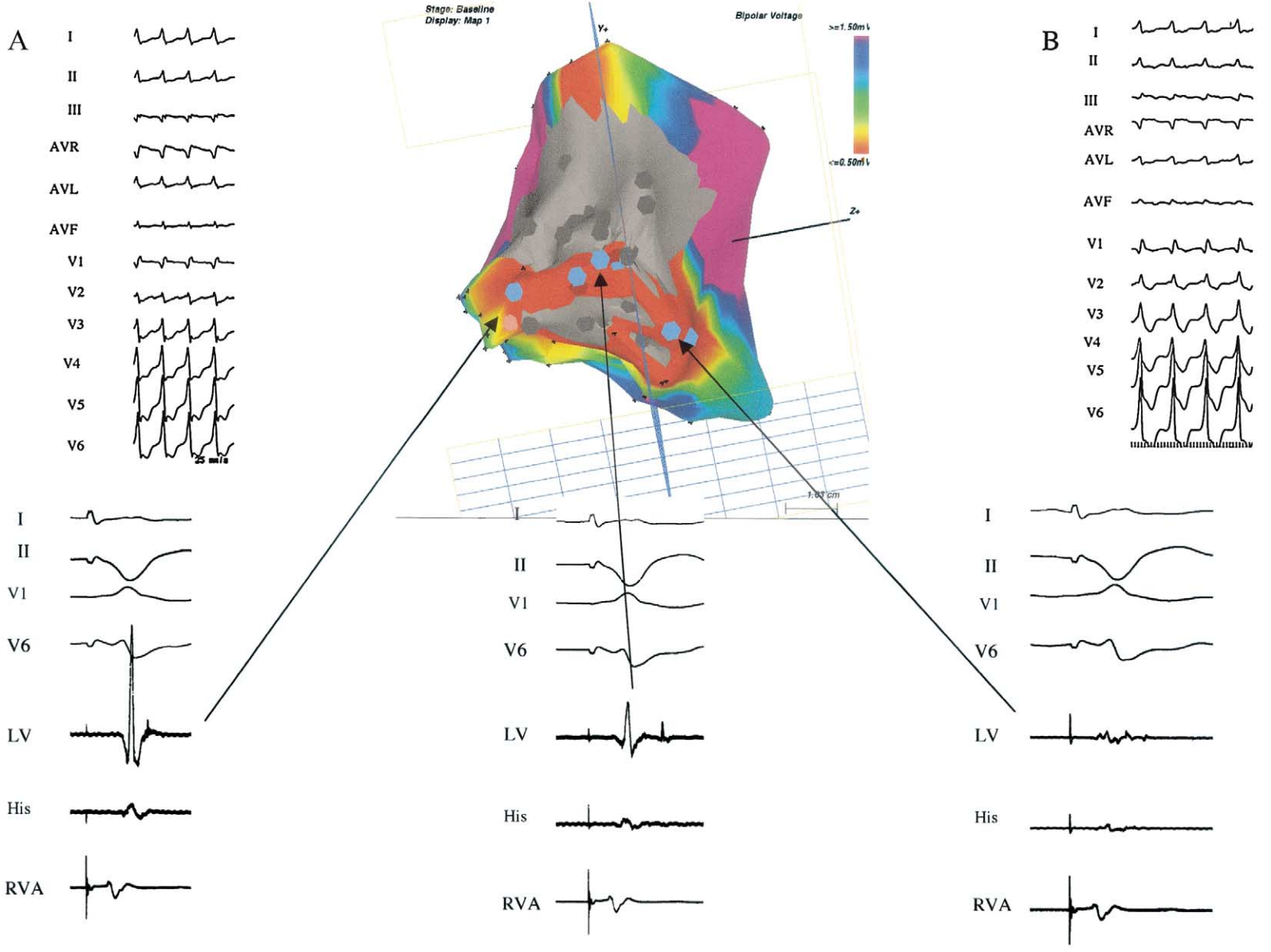

Figure 3. Voltage map showing the location of the E-IDC area. This map during RVA pacing shows a right and inferior view of the septum and inferior walls of the left ventricle (LV) in a patient with ischemic heart disease. The color range represents the voltage amplitude. **Red** denotes dense scar, and **gray** denotes complete scar. **Blue dots** show sites where E-IDCs surrounded by complete scar were recorded. The **arrows** show the electrogram recorded at the entrance of the corridor **(pink dot)**, at the E-LIDC site, and at the site where multiple components were recorded. **Red dots** denote the E-IDC sites where radiofrequency energy was delivered. **(A)** Clinical VT. **(B)** Pace map from the E-LIDC reproducing the VT morphology with a long S-QRS interval.

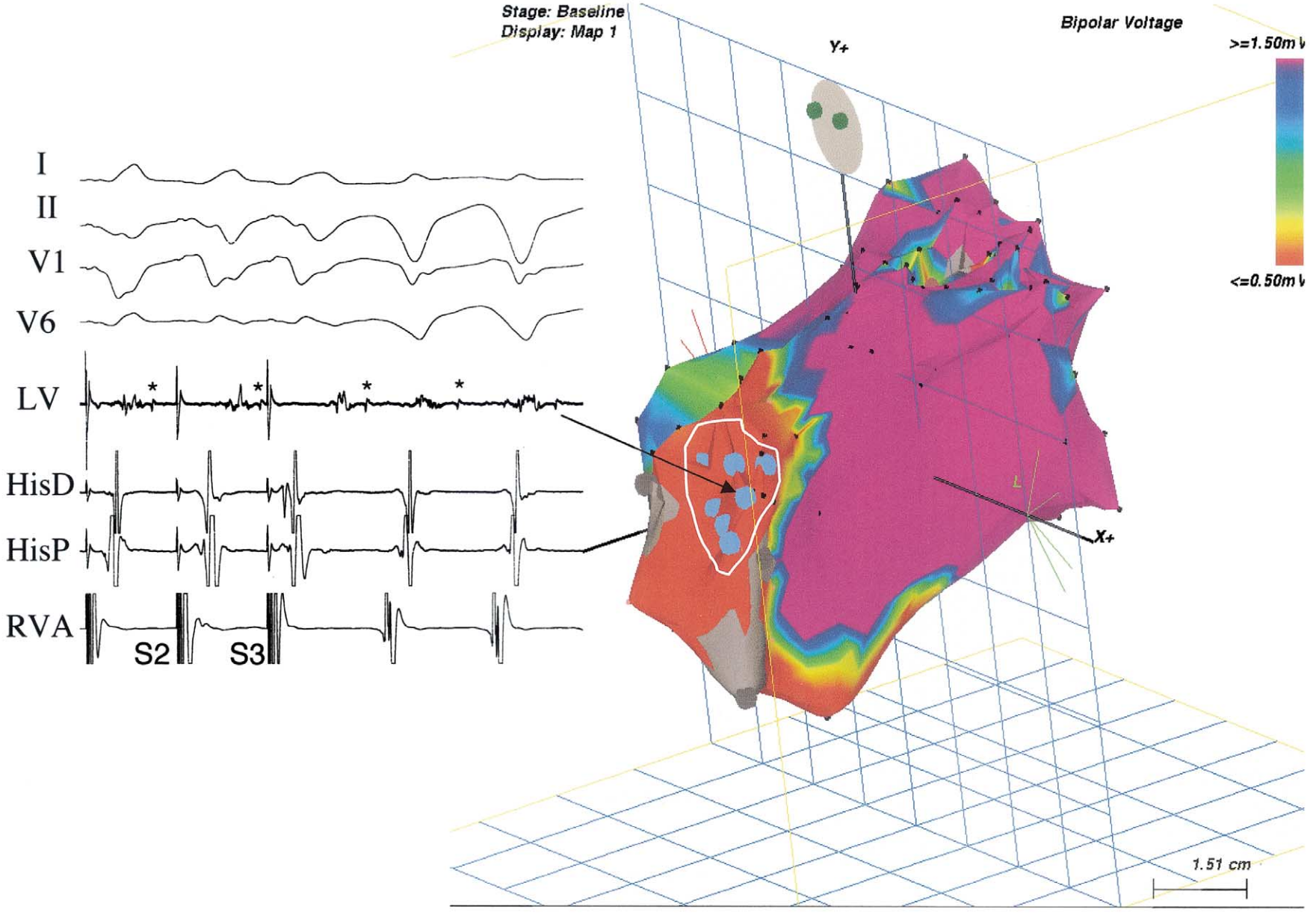

Figure 4. Induction of VT from the RVA during the recording of E-ILDC. **(A)** Four ECG surface leads and intracardiac recordings from the His area, RVA, and left ventricle (LV) are recorded during RVA pacing. The introduction of two extrastimuli provoked the lengthening of the activation time of the E-LIDC and the induction of VT. The E-LIDC preceded the first VT beat and became mid-diastolic. **(B)** Voltage map showing all E-IDC sites of the area **(blue dots)**.

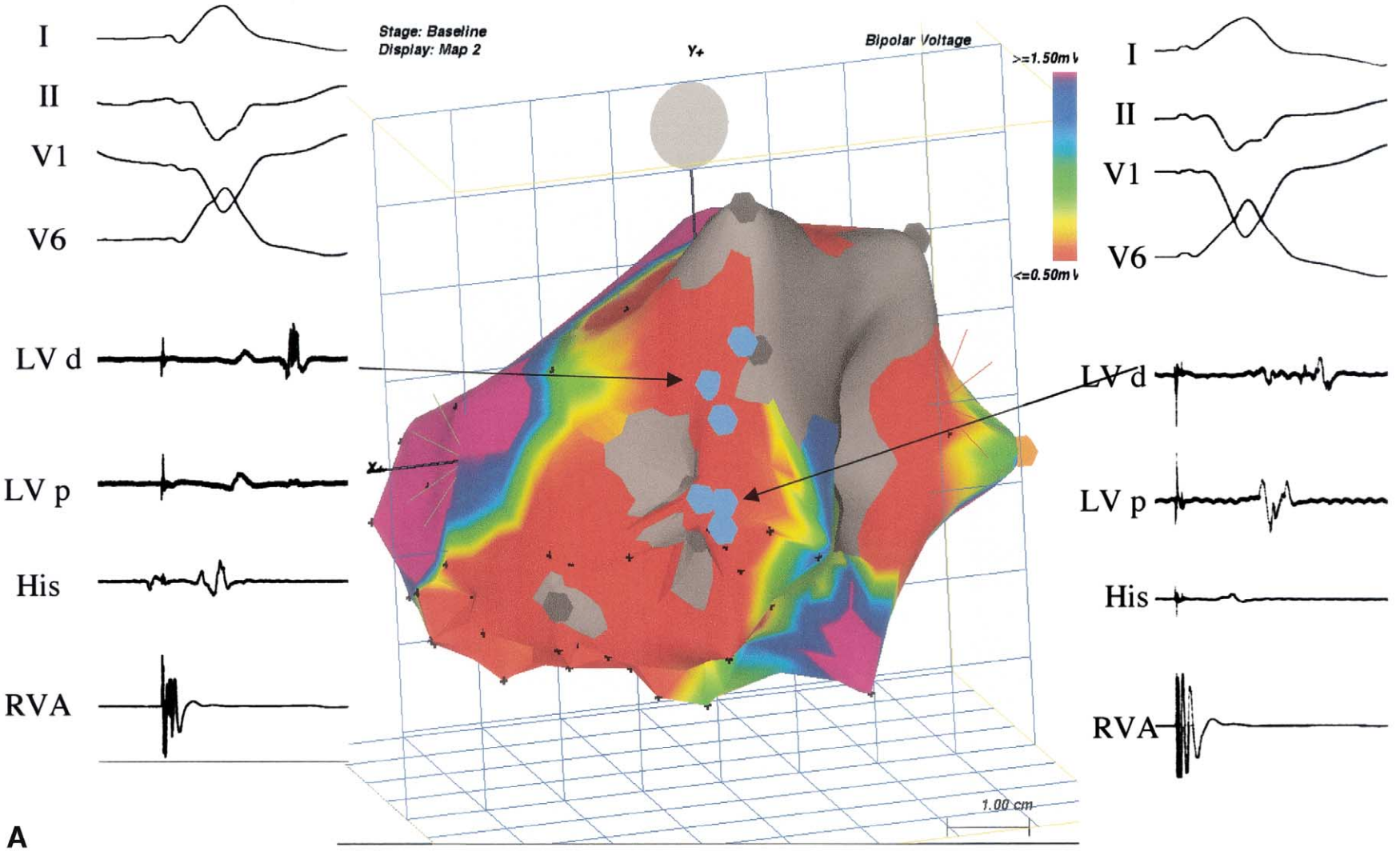

Figure 5. **(A)** Voltage map obtained during RVA pacing. The E-IDCs were recorded in the space located between the inferior and superior scars. *Continued on next page.*

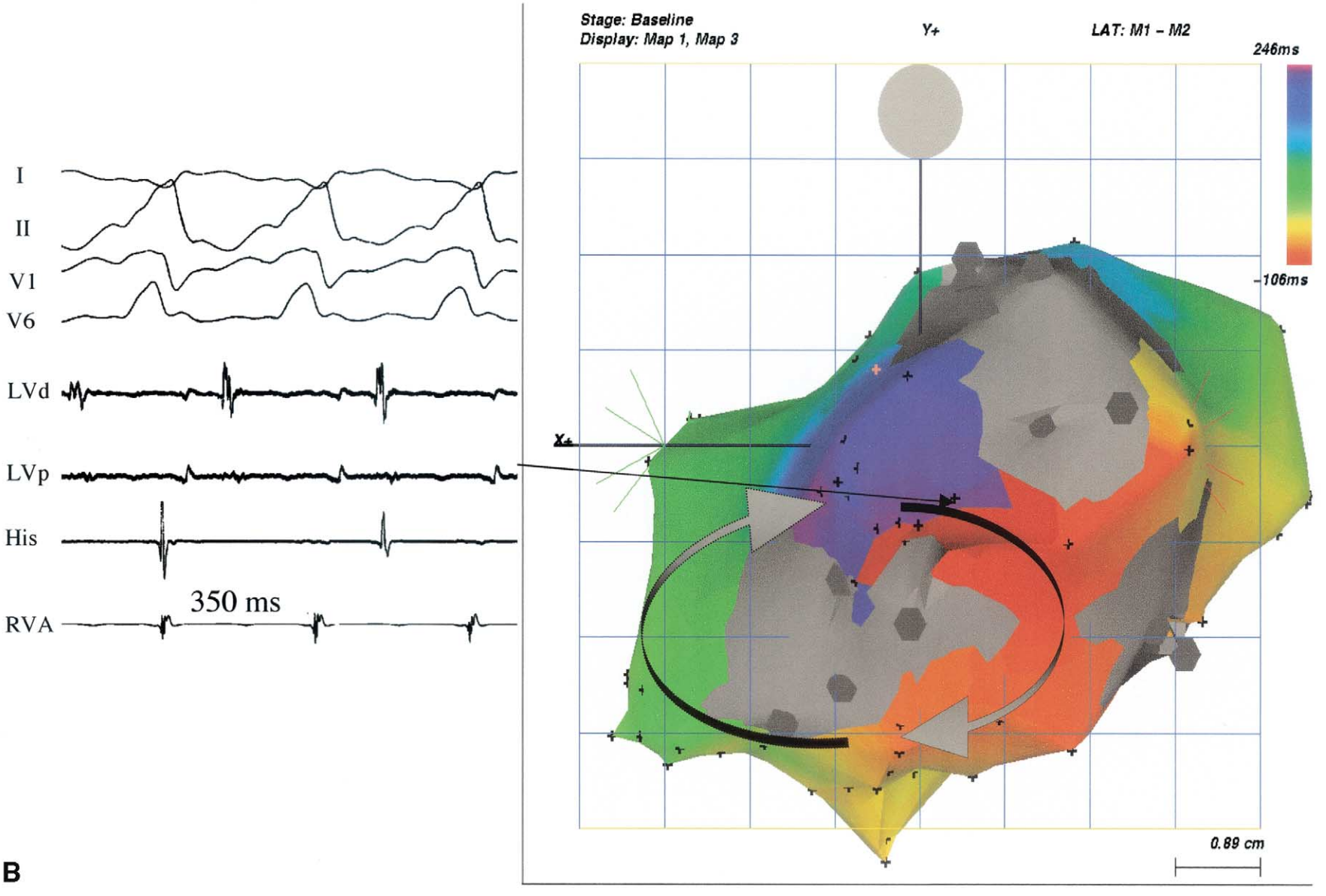

Figure 5 Continued. (B) Activation map recorded during VT. The color index reveals the continuity between the earliest and latest activated areas typical of reentry. The E-IDC during RVA pacing and mid-diastolic electrogram of VT have the same morphology and are recorded at the same site. LV = left ventricle.

Table 3. Ablation Guidance and Recurrences During Follow-Up

Patient No.	Ablation Site Guidance	Follow-Up (months)	Recurrences (no. of episodes)
1	E-IDC	17	0
2	E-IDC	4	0
3	E-IDC	16	0
4	E-IDC	9	1
5	E-IDC	12	0
6	E-IDC	12	0
7	E-IDC	12	VF
8	E-IDC	11	0
9	E-IDC	10	0
10	E-IDC	12	0
11	E-IDC	12	0
12	E-IDC	12	0
13	E-IDC	10	0
14	E-IDC	19	1 (different VT)
15	E-IDC	7	0
16	E-IDC	7	0
17	E-IDC	2	2 (different VT)
18	E-IDC	7	multiple
19	C-EM	7	multiple
20	C-EM	12	0
21	C-EM	6	0
22	C-EM	10	0
23	C-EM	7	0
24	C-EM	5	0

C-EM = conventional entrainment-mapping; E-IDC = electrograms with isolated, delayed component; VF = ventricular fibrilation; VT = ventricular tachycardia.

voltage ≤0.5 mV, including complete and dense scar (22 ± 11 cm^2 [range 11 to 50]; $p < 0.01$) (Fig. 3). The E-IDCs were recorded close to the border but inside the dense scar. The minimum distance from the limit of the E-IDC area to the border of the scar, defined by the distance to the closest electrogram of >0.5 mV, was 1.6 ± 0.6 cm. The voltage of the E-LIDC was 0.26 ± 0.11 mV (range 0.11 to 0.5), which was similar to the voltage of the electrogram recorded at the sites where VT was successfully ablated (0.27 ± 0.11 mV [range 0.1 to 0.5]; p = 0.5 [NS]). The maximum voltage recorded inside the E-IDC areas was 0.41 ± 0.23 mV (range 0.19 to 1.2).

Relationship between E-IDC and clinical VT. From a total of 29 E-IDC areas, 24 were related to documented clinical VTs (Table 2).

In the 18 patients (Patient nos. 1 to 18) with unmappable VT, 22 of 24 recorded clinical VTs could be related to the E-IDC areas. Fifteen VTs in 15 patients were reproduced during pace mapping from the E-LIDC (S-QRS interval 110 ± 45 ms) (Fig. 3). Four additional VTs were reproduced from the limits of the E-IDC area. Three more clinical VTs, despite a different pace map, could be related to the E-IDC by the fact that during VT induction, the E-LIDC preceded the first VT beat and then became mid-diastolic (Fig. 4). Two tachycardias—morphologies of right bundle branch block left superior axis in Patient no. 2 and right bundle branch block right inferior axis in Patient 4—could not be related to the E-IDC area. In five patients in whom the pace map and the induced VTs were identical, the difference between the S-QRS and E-QRS was 8 ± 8 ms, suggesting that these electrograms were near the central isthmus of the circuit. In this group, three induced VTs, different from the target clinical VT, were tolerated and mapped, as no mid-diastolic electrogram was recorded outside the E-ICD area; the RFA approach was not modified. Among the six patients with clinically inducible and well-tolerated VT, three had successful ablation sites that were undoubtedly inside the E-IDC area, and in two other patients, these sites were just within the limits of the E-ICD area (20 and 16 mm away from the E-LIDC). In one patient, we could not ablate the VT. Complete activation maps during VT were obtained in three patients. In one of these cases, we identified during RVA pacing a slow conduction area connecting the E-IDC recorded between two scar areas. During tachycardia, this area functioned as the central pathway of the circuit (Fig. 5).

Ablation results and duration of procedure. Between 1 and 35 (11 ± 8) RFA lesions were applied per patient. In patients with unmappable VT, from 3 to 12 (6 ± 2) IDC sites were ablated using from 3 to 35 (13 ± 8) RFA lesions. Previously inducible VT became noninducible in all but patient no. 19. Inducibility suppression was not tested in Patients 12 and 17 because of hemodynamic instability. After the ablation procedure, ventricular fibrillation was induced in Patients 8 and 15, and a fast, nonclinical VT was induced in Patients 7, 9, 16, 23, and 24. The total procedure time ranged from 142 to 448 min (mean 232 ± 67). The total fluoroscopy time ranged from 25 to 105 min (mean 56 ± 28). There were no complications during the procedure.

After the RFA procedure, three additional patients received an ICD (Patients 4, 7, and 8). Despite the fact that some VTs were not inducible or nonsuppressed, Patients 2, 17, and 19 were not considered as candidates to receive an ICD, based on their very short life-expectancy. Patients 9 and 16 with noninducible VT refused an ICD implant.

Follow-up (Table 3). During the follow-up period of 9 ± 4 months, four patients died. Three patients (Patients 2, 17, and 19) died of congestive heart failure. These patients were in functional class III/IV before the ablation procedure. Patient 21 died of a noncardiac cause six months after ablation, without recurrence of VT. Patient 7 had ventricular fibrillation treated by the defibrillator. Five patients had VT recurrences. The morphology of the VT recurrence was different from the previous clinical VT in Patients 14 and 17. Patients 4, 18, and 19 had recurrences of clinical VT.

DISCUSSION

Unmappable VTs are still considered a limitation of RFA, and no definitive approach has been widely accepted. Marchlinski et al. (16) recently described a method in which identification of the scar and exit site by means of pace mapping was used to decide where to create lines of ablation to treat unmappable VT in patients with chronic myocardial infarction and arrhythmogenic right ventricular dysplasia.

We describe a new method of treatment of monomorphic VT that can be feasibly applied to patients with unmappable VT. This method is based on the recording of electrograms that identify slow conduction areas during SR and RVA pacing. This method overcomes the limitations detected in previous studies, in which the recording of simply abnormal low-voltage electrograms was highly nonspecific due to the extensive areas in which they were located (9). The criterion we selected for identification of the VT substrate was based on the observation that late and long-duration electrograms, despite a low sensitivity, were highly specific for VT circuit identification (10); this criterion also required the recording of high-frequency electrograms with multiple components separated by an isoelectric line, similar to the electrograms recorded at the central common pathways or adjacent bystander (17). This type of electrogram, although unable to differentiate the central isthmus from a closed bystander, reduced the area of interest, increasing the specificity, as can be appreciated when voltage maps are studied. It is important to notice that RVA pacing permitted the identification of the VT substrate in several patients in whom the SR map was not sensitive enough, supporting our hypothesis that a change in the direction of the activation front might unmask some areas of block and slow conduction. These data are in agreement with those reported previously by Brunckhorst et al. (18), in which multipotential electrograms with >2 deflection, highly predictive of a reentrant circuit, were more frequently recorded during right ventricular pacing. Moreover, we can speculate that during SR, several simultaneous activation wave fronts may coexist, making the probability of electrogram overlap higher than during RVA pacing, when only one activation wave front is present.

Location of E-IDC. Voltage maps showed that E-IDC areas were located inside the dense scar tissue. These results are compatible with those obtained during surgical treatment of VT in which the electrogram recorded at sites related to VT had a voltage amplitude <0.5 mV (19), as well as with those data more recently reported in which the fractionated electrograms were always recorded in dense scar (20).

Advantages of ablation of E-IDC areas. The E-IDC areas are relatively small compared with scar areas; therefore, this method permits a focus on the diagnostic techniques and ablation in defined areas. This procedure allows the ablation of some nontolerated VTs not approachable by conventional entrainment mapping, as: 1) the recording of E-IDC before and during VT induction serves to relate E-IDCs and VT within seconds, provided that the IDC precedes the first VT beat and then becomes mid-diastolic; and 2) the ablation of all IDC sites overcomes the lack of specificity of the selection of a single site as an ablation target when entrainment mapping criteria are not fulfilled. Ablation of these electrograms could also eliminate the substrate for different VTs otherwise not ablated by limited conventional strategies.

Study limitations. In patients with inducible and nontolerated VT, we could not differentiate between the E-IDC recorded in the central common pathway of the circuit from those recorded in areas probably connected but not related to the VT circuit, as an adjacent bystander. Nevertheless, isolated potentials are usually recorded near the central common pathway (17). In few patients with more than one clinical VT, not all VTs could be related to the E-IDC areas; a nonendocardial circuit and the complexity of some circuits in which several exit sites coexist might preclude the reproduction of certain morphologies. Moreover, this treatment strategy has not proven its efficacy in patients with nontolerated and undocumented VTs, mainly when these patients have more than one E-IDC area. In patients with a low frequency of episodes, it is not possible to determine the long-term efficacy of the procedure. A reduction in ventricular function was not systematically evaluated; nevertheless, no clinical deterioration related to the procedure was observed.

Reprint requests and correspondence: Dr. Angel Arenal, Laboratorio de Electrofisiología, Departamento de Cardiología, Hospital General Universitario Gregorio Marañón, C/Dr. Esquerdo 46, 28007 Madrid, Spain. E-mail: arenal@doymanet.es.

REFERENCES

1. de Bakker JM, van Capelle FJ, Janse MJ, et al. Reentry as a cause of VT in patients with chronic ischemic heart disease: electrophysiologic and anatomic correlation. Circulation 1988;77:589–606.
2. Stevenson WG, Khan H, Sager P, et al. Identification of reentry circuit sites during catheter mapping and radiofrequency ablation of ventricular tachycardia late after myocardial infarction. Circulation 1993;88:1647–70.
3. Bogun F, Bahu M, Knight BP, et al. Comparison of effective and ineffective target sites that demonstrate concealed entrainment in patients with coronary artery disease undergoing radiofrequency ablation of ventricular tachycardia. Circulation 1997;95:183–90.
4. Rothman SA, Hsia HH, Cossu SF, Chmielewski IL, Buxton AE, Miller JM. Radiofrequency catheter ablation of postinfarction ventricular tachycardia, long-term success, and the significance of inducible nonclinical arrhythmias. Circulation 1997;96:3499–508.
5. Kay GN, Epstein AE, Plumb VJ. Regions of slow conduction in sustained ventricular tachycardia: direct endocardial recordings and functional characterization in humans. J Am Coll Cardiol 1988;11:109–16.
6. Kim YH, Sosa-Suarez G, Trouton TG, et al. Treatment of ventricular tachycardia by transcatheter radiofrequency ablation in patients with ischemic heart disease. Circulation 1994;89:1094–102.
7. Fitzgerald DM, Friday KJ, Wah JA, Lazzara R, Jackman WM. Electrogram patterns predicting successful catheter ablation of ventricular tachycardia. Circulation 1988;77:806–14.
8. Strickberger SA, Man KC, Daoud EG, et al. A prospective evaluation of catheter ablation of ventricular tachycardia as adjuvant therapy in patients with coronary artery disease and an implantable cardioverter-defibrillator. Circulation 1997;96:1525–31.
9. Cassidy DM, Vassallo JA, Miller JM, et al. Endocardial catheter mapping during sinus rhythm: relation of underlying heart disease and ventricular arrhythmia. Circulation 1986;73:645–52.
10. Cassidy DM, Vassallo JA, Marchlinski FE, Buxton AE, Untereker WJ, Josephson ME. Endocardial mapping in humans in sinus rhythm with normal LVs: activation patterns and characteristics of electrograms. Circulation 1984;70:37–42.
11. Otomo K, Gonzalez MD, Beckman KJ, et al. Reversing the direction of paced ventricular and atrial wavefronts reveals an oblique course in

accessory AV pathways and improves location for catheter ablation. Circulation 2001;104:550–6.
12. Shah D, Haissaguerre M, Jais P, et al. Left atrial appendage activity masquerading as pulmonary vein potentials. Circulation 2002;105: 2821–5.
13. Arenal A, Almendral JM, Alday J, et al. Rate-dependent conduction block of the crista terminalis in patients with typical atrial flutter: influence on the evaluation of cavotricuspid isthmus conduction block. Circulation 1999;99:2771–8.
14. Gepstein L, Hayam G, Ben-Haim SA. A novel method for non-fluoroscopic catheter-based electroanatomical mapping of the heart: in vitro and in vivo accuracy results. Circulation 1997;95:1611–22.
15. Shpun S, Gepstein L, Hayam G, Ben-Haim SA. Guidance of radio-frequency endocardial ablation with real-time three-dimensional magnetic navigation system. Circulation 1997;96:2016–21.
16. Marchlinski FE, Callans DJ, Gottlieb CD, Zado E. Linear ablation lesions for control of unmappable ventricular tachycardia in patients with ischemic and nonischemic cardiomyopathy. Circulation 2000; 101:1288–96.
17. Kocovic DZ, Harada T, Friedman PL, Stevenson WG. Characteristics of electrograms recorded at reentry circuit sites and bystanders during ventricular tachycardia after myocardial infarction. J Am Coll Cardiol 1999;34:381–8.
18. Brunckhorst CB, Stevenson WG, Jackman WM, et al. Ventricular mapping during atrial and ventricular pacing: relationship of multipotential electrograms to ventricular tachycardia reentry circuits after myocardial infarction. Eur Heart J 2002;23:1131–8.
19. Josephson ME, editor. Recurrent ventricular tachycardia. In: Clinical Cardiac Electrophysiology: Techniques and Interpretation. 2nd ed. Philadelphia, PA: Lea & Febiger, 1993:417–615.
20. Callans DJ, Ren JF, Michele J, Marchlinski FE, Dillon SM. Electroanatomic left ventricular mapping in the porcine model of healed anterior myocardial infarction: correlation with intracardiac echocardiography and pathological analysis. Circulation 1999;100:1744–50.